Examination of the Surface Energy Budget: A Comparison of Eddy Correlation and Bowen Ratio Measurement Systems

JERALD A. BROTZGE* AND KENNETH C. CRAWFORD

Oklahoma Climatological Survey, University of Oklahoma, Norman, Oklahoma

(Manuscript received 5 June 2001, in final form 29 August 2002)

ABSTRACT

A reliable method for monitoring the surface energy budget is critical to the development and validation of numerical models and remote sensing algorithms. Unfortunately, closure of the energy budget remains difficult to achieve among measurement systems. Reasons for nonclosure still are not clearly understood, and, until recently, few long-term datasets were available to address this issue of nonclosure. This contribution examined 108 days of a year dataset collected from collocated eddy correlation (EC) and Bowen ratio (BR) systems. Differences between systems were examined across seasonal and diurnal cycles to better understand nonclosure of the energy budget. Closure by the EC system was observed to vary with season and with time of day, primarily as a function of latent heat flux. Furthermore, the EC and BR methods partitioned energy differently, with the EC system favoring latent heat flux and the BR system favoring sensible heat flux.

Instrument error, surface heterogeneity, and the theoretical assumptions behind the EC and BR methods are discussed to explain observed patterns in closure and the differences between measurement systems. Sensor error and variability in net radiation and soil moisture data increased uncertainty in measurements of net radiation and ground heat flux. Significant differences in soil temperature and flux between sites appear to be caused by the heterogeneity of vegetation and soil type. Finally, several assumptions of the BR method are examined to explain observed differences in sensible and latent heat flux between systems. Recommendations for future observational studies are proposed.

1. Introduction

The net radiation (R_n) at the earth's surface (assuming no snow cover) is either absorbed into the ground in the form of ground heat flux (G), or transferred to the atmosphere in the form of sensible (H) and latent heat (LE) flux. Closure (i.e., $R_n - H - \mathrm{LE} - G = 0$) is one tool used to quantify the reliability and accuracy with which these components of the surface energy budget are measured. Unfortunately, most field measurements have failed to show closure of the surface energy budget (McNeil and Shuttleworth 1975; Dugas et al. 1991; Fritschen et al. 1992; Stannard et al. 1994; Lloyd et al. 1997; Twine et al. 2000). Instrument error, changes in surface heterogeneity, and fetch can affect measurements of closure of the surface energy balance.

One way to identify systematic problems associated with closure is to evaluate the performance of collocated, independent measurement systems. Eddy correlation (EC) and Bowen ratio (BR) methods are two such independent systems for measuring surface fluxes. Eddy correlation directly measures the eddy covariances of fluxes and provides independent measurement of all four components of the energy budget. The disadvantages of EC include sensitivity to fetch and high cost and maintenance requirements. The BR system requires less maintenance and is generally cheaper; however, closure is forced, and the eddy diffusivities of heat and moisture must be assumed equal.

McNeil and Shuttleworth (1975) were among the first to compare the EC and BR methods. Examining flux measurements above a pine forest, they found a difference in H that was ~24% less by the EC method when compared to the BR technique. Dugas et al. (1991) conducted a similar comparison over an irrigated wheat field to minimize surface heterogeneity. Still, the results were not unlike those found by McNeil and Shuttleworth (1975) and Shuttleworth et al. (1984); the EC estimates of H were 18% and 31% less than those from the BR technique on two successive days of comparison. Estimates of LE from the EC were 23% and 33% less than those from the BR system.

During the late 1980s and 1990s, several large field projects investigated the closure issue. Results from the First International Satellite Land Surface Climatology

* Current affiliation: Center for Analysis and Prediction of Storms, University of Oklahoma, Norman, Oklahoma.

Corresponding author address: Dr. J. A. Brotzge, Center for Analysis and Prediction of Storms, University of Oklahoma, 100 E. Boyd, Suite 1110, Norman, OK 73019.
E-mail: jbrotzge@ou.edu

Project (ISLSCP) Field Experiment (FIFE) repeated those of previous studies: the EC method measured smaller aerodynamic fluxes (H + LE) when compared to BR estimates (Sellers and Hall 1992). One such comparison used a one-dimensional sonic anemometer to determine that EC underestimated (H + LE) by as much as 24% (Fritschen et al. 1992).

In a comprehensive study of the issue, Twine et al. (2000) examined the closure of the surface energy budget during June and July of the Southern Great Plains '97 (SGP-97) Hydrology Experiment. Both EC and BR measurements were acquired at 11 sites across the SGP-97 region. Closure rates for the EC systems ranged between 67% and 83%. Residuals of the energy budget were greater than 100 W m^{-2} (J. Norman 1999, personal communication). Despite problems with closure, EC remains the *only* tool for direct measurement of LE and *H*. It is clear, from numerous studies documented in the scientific literature, that reasonable closure of the surface energy budget remains an elusive problem.

Generally, these previous efforts have been limited to data collected during a relatively short period of days to several months whereas a longer period of comparison is needed to adequately quantify instrument and seasonal bias and trends associated with a measurement site. The purpose of this research is to examine a long-term comparison between an eddy correlation and Bowen ratio system to better identify problems associated with closure of the surface energy budget. Section 2 reviews the instrumentation used in this study. Section 3 quantifies the daily closure rates observed by the EC method compared to the BR technique. Seasonal and diurnal trends in closure estimates also are examined. Problems with measurement of the available energy components, R_n and G, are examined in section 4. Section 5 discusses theoretical assumptions and surface heterogeneity as possible sources of closure error, especially with respect to the aerodynamic fluxes LE and *H*.

2. Description of the instrumentation and measurement techniques

a. Data and site information

The Oklahoma Mesonet (Brock et al. 1995) is a statewide network of 115 meteorological stations. Each site measures solar radiation, atmospheric pressure, precipitation, wind speed and direction at 10 m, air temperature and relative humidity at 1.5 m, and bare soil and sod temperature at 10-cm depth. Data are averaged every 5 min and collected in real time on a continuous basis. During 1999, the Oklahoma Atmospheric Surface-Layer Instrumentation System (OASIS) Project (Brotzge et al. 1999) instrumented 10 mesonet sites (Fig. 1) with four-component net radiometers, ground heat flux sensors, and EC instrumentation. One of these 10 OASIS sites is the mesonet site at Foraker and is collocated with an Atmospheric Radiation Measurement (ARM) Energy Balance Bowen Ratio (EBBR) system.

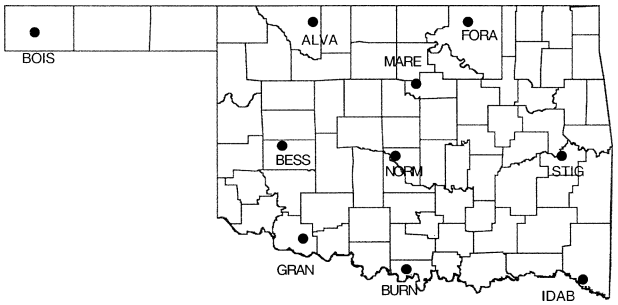

FIG. 1. Map of the ten OASIS super sites which are equipped with net radiation, ground heat flux, and eddy correlation instrumentation. The ARM site is collocated with the mesonet site facility at Foraker (FORA) in northeastern Oklahoma.

The ARM Program (Stokes and Schwartz 1994) is a global research program supported by the Department of Energy. One of three primary research sites is the Southern Great Plains (SGP) Cloud and Radiation Testbed (CART) region spanning over 122 000 km^2 across portions of south-central Kansas and north-central Oklahoma. The SGP–CART region includes 14 EBBR sites.

The ARM EBBR site at Foraker is approximately 100 m north-northwest of the mesonet EC tower, which allows measurements of the energy budget to be compared between these two ''collocated'' sites. The EBBR site, located at ~36°50′25″N latitude and 96°25′40″W longitude, is a so-called extended facility site of the ARM Program, which began operating in June 1995. The site slopes downward from south to north, and the EBBR site is approximately 1–2 m lower in elevation than is the mesonet EC site. The site is located in the Tallgrass Prairie Preserve in north-central Oklahoma. Buffalo graze on much of the nearby land. Vegetation cover is classified by ARM as 80%–90% weeds and 10%–20% Johnson grass. The weeds typically reach 1.0 m in height, and grasses commonly grow to 2.0 m in height. The prairie has a thick vegetation cover, and a visual inspection showed no discernible differences in vegetation between the EC and EBBR sites. Soil type at the EBBR site is classified by the State Soil Geographic Database (STATSGO) as silt loam. Soil directly sampled from the EC site is classified as sandy loam at 5 and 25 cm and sandy clay loam at 60 and 75 cm.

b. Instrumentation

A list of the instrumentation used by this study is summarized in Table 1. An automated system for data processing applied all calibrations and appropriate corrections to the data (Brotzge et al. 2001). A brief description of the measurement techniques and assumptions used is provided below.

TABLE 1. Summary of instrumentation.

	Mesonet/OASIS (EC)	ARM (EBBR)
Four-component radiation	CNR1	SIRS
Net radiation only	NR-Lite	*Q**6.1
Ground heat flux	Two HFT3.1 ground flux plates installed at 5-cm depth	Five HFT3.1 ground flux plates installed at 5-cm depth
	Two REBS platinum resistance temperature detectors (PRTDs) installed at 0–5-cm depth, spaced 1.0 m apart	Five REBS PRTDs installed at 0–5-cm depth, spaced 1.0 m apart
Sensible heat flux	CSAT3 sonic anemometer	Bowen ration system; vertical temperature/moisture gradient measured between 2 and 3 m
Latent heat flux	KH-20 Krypton hygrometer	
Soil moisture	One resistance-type 229-L sensor, installed at 5-cm depth, spaced 1.0 m apart	(EBBR) five resistance-type SMP-2 sensors, installed at 2.5-cm depth, spaced 1.0 m apart (SWATS) two resistance-type 229L sensors, installed at 5-cm depth, spaced 1.0 m apart

1) NET RADIATION

Net radiation remains among the most difficult atmospheric parameters to measure accurately. The foremost problem in observing net radiation properly is the absence of a World Meteorological Organization (WMO) standard for longwave radiation (Ohmura et al. 1998). Because of the lack of a uniform standard, calibrations of net radiometers vary greatly among instrument companies and among model types (e.g., Field et al. 1992). In addition, radiation error can be caused by the cosine response, wind speed, and precipitation effects.

The EC system measures net radiation using the CNR1 radiometer manufactured by Kipp & Zonen to measure each of the four components of R_n. The site also is equipped with a domeless net radiometer, termed the NR-Lite, also manufactured by Kipp & Zonen. Both sensors are mounted at a height of 2 m. The EBBR site measures radiation using a Solar Infrared Radiation Station (SIRS) system. The SIRS consists of four individual sensors—upward and downward facing pyranometers (PSPs) and pyrgeometers (PIRs), all manufactured by the Eppley Laboratory, Inc. The manufacturer lists calibration uncertainty as ±2% for PIRs and ±3% for PSPs. Total net radiation also is measured at the EBBR sites using a domed model *Q**6.1 manufactured by Radiation and Energy Balance Systems (REBS). All EBBR (SIRS) radiation sensors are mounted at a height of 2.6 m (2.0 m).

The SIRS and CNR1 radiometers measure each component of the radiation budget explicitly and are considered more accurate instruments for observing net radiation than either the *Q**6.1 or NR-Lite sensors. Because the CNR1 also is used for closure of the energy budget, a critical issue is the accuracy with which net radiation is measured.

2) SENSIBLE AND LATENT HEAT FLUXES

Sensible and latent heat fluxes at the EC site were estimated directly using a CSAT3 sonic anemometer and KH-20 Krypton hygrometer, manufactured by Campbell Scientific, Inc. (CSI). Both sensors were installed at a height of 4.5 m and sample at a rate of 8 Hz. Eddy correlation estimates (Kaimal and Gaynor 1991) of H are a function of specific humidity and were corrected according to Schotanus et al. (1983). The specific heat of air, C_p, varies as a function of moisture and was corrected as given by Stull (1988). Latent heat was corrected for the effects of density fluctuations as explained by Webb et al. (1980). Estimates of LE from the krypton hygrometer vary as a function of the density of oxygen in the air and were corrected as defined by Tanner et al. (1993). In addition, coordinate rotation was applied to all EC estimates to correct for tilt of the sonic anemometer.

The EBBR system used by ARM directly measures vertical gradients of temperature and relative humidity. Latent heat is estimated as a function of the Bowen ratio,

$$\mathrm{LE} = \frac{R_n - G}{1 + \beta}. \tag{1}$$

The Bowen ratio (β) is estimated from the vertical gradients of temperature (T_1, T_2) and specific humidity (q_1, q_2) at two heights. The Bowen ratio is calculated as

$$\beta = \frac{C_p}{L_v}\frac{K_h}{K_w}\frac{(T_1 - T_2)}{(q_1 - q_2)} = \frac{H}{\mathrm{LE}}, \tag{2}$$

where C_p is the specific heat of dry air, L_v is the latent heat of vaporization, and K_h and K_w are the eddy diffusivities for heat and water vapor, respectively (Ohmura 1982). The eddy diffusivities are assumed to be equal. Sensible heat is estimated as the residual of the energy budget. Vertical gradients in air temperature and moisture are measured using temperature and humidity sensors mounted at heights of 2 and 3 m. An automatic exchange mechanism switches the two temperature and humidity sensors vertically every 15 min to minimize systematic error due to instrument offset and drift. The average of data produced by two 13-min averages of 30-s samples yields a final 30-min mean of H and LE.

3) Ground heat flux

The surface ground heat flux across the top of an uppermost soil layer, of given depth, is given by the sum of the heat flux across the bottom of the soil layer and the storage of heat within the layer. Tanner (1960) developed a ''combination approach'' for measuring surface ground heat flux that includes separate measurements of 1) the heat flux at the bottom of the layer and 2) the heat storage within the layer. Thus, Tanner derives the ground heat flux from (see derivation in the appendix)

$$G = -\lambda \left.\frac{dT}{dz_1}\right|_{z_2} + z_2 \overline{\left(C\frac{dT}{dt}\right)}^{z_2}, \quad (3)$$

where dT/dz_1 is the temperature gradient (K m^{-1}) across a heat flux measuring plate of thickness dz_1 placed at soil depth z_2, λ is the soil thermal conductivity [W (m K)$^{-1}$] at the depth z_2, C [J (m^3 K)$^{-1}$] is the soil heat capacity, and dT/dt (K s^{-1}) is the temporal rate of change of soil temperature, and the overbar denotes the vertical integral over the depth z_2 of the soil layer. Assuming C is invariant over depth z_2, then

$$G = -\lambda \left.\frac{dT}{dz_1}\right|_{z_2} + z_2 C\left(\frac{d\overline{T}}{dt}\right). \quad (4)$$

At the EC site, two soil heat flux plates, REBS' model HFT-3.1s, are installed at a depth of 5 cm, and the average of the data from the two plates is used to estimate the first term in Eq. (4). Two platinum resistance temperature detectors (PRTDs), also manufactured by REBS, are installed diagonally at 0 to 5 cm, and the mean of the data from the two PRTDs is used to calculate dT/dt in the second term of Eq. (4). The soil heat capacity, C, is estimated as a function of the measured volume fraction of minerals, organic matter, and soil moisture. Ground heat flux estimates at the EC site are corrected for differences between plate and soil thermal conductivities as described by Fritschen and Simpson (1989). Note that the soil conductivity, λ, as used in term (1) of Eq. (4) is the plate conductivity and does not depend on soil moisture.

At the EBBR facility, the heat flux at the bottom of the soil layer was estimated as the average of data from five soil heat plate sensors, which like the EC site, are REBS' HFT-3.1s and are buried at a depth of 5 cm. The ground heat storage term was calculated as a function of the soil heat capacity (computed as a function of soil moisture, estimated at a depth of 2.5 cm) and the integrated soil temperature as observed from five REBS' PRTDs buried between 0 and 5 cm.

A number of errors can occur when attempting to estimate ground heat flux (Massman 1993). For example, significant error occurs when the thermal conductivity of the flux plate sensor at the bottom of the soil layer does not match the conductivity of the soil. Another complication develops when the flux plate itself impedes the vertical flow of heat and moisture within the soil. Air gaps between the flux plate and soil can also increase measurement error. Finally, surface heterogeneity in soil type, soil moisture, and vegetation severely limit the spatial representativeness of the point measurement.

4) Soil moisture

Soil heat capacity is primarily a function of the soil moisture, and so the accuracy of ground heat flux measurements is critically dependent upon the measurement of soil moisture. The ARM EBBR facility estimates the percent soil water (ratio of the mass of soil water to the mass of dry soil) from the soil water potential measured from five resistance-type soil moisture sensors, a model SMP-2 manufactured by REBS. An average data value from the five sensors is used. The ARM facility also is equipped with the Soil Water and Temperature System (SWATS), a second independent measurement of soil moisture. SWATS measures the soil water potential directly using the average of two 229L sensors, manufactured by CSI. The EC site measures soil water potential using a single 229L sensor. Both SWATS and EC estimates of soil water potential are converted to volumetric water content (ratio of volume of soil water to volume of total soil) using empirical soil water retention curves, which are unique to each site. The single EC soil moisture sensor is installed at a depth of 5 cm; the two soil moisture sensors at EBBR (SWATS) are installed 1 m apart at a depth of 2.5 cm (5.0 cm). All soil moisture observations were acquired at 30-min intervals.

c. Data quality control

All EC and EBBR calculations used 30-min data; when 5 or more of the 48 observations were missing, that day of data was excluded. If fewer than five observations were missing, data were linearly interpolated to complete the time series. Several large gaps in the data record appear due to inoperable sensors. SIRS radiation data were unavailable between 1 June and 31 August 1999. Radiation data collected from the EC NR-Lite sensor were unavailable during 8 August–7 September, 1999. The krypton hygrometer at Foraker was out of order during 29 October 1999–3 February 2000, and so H and LE data from the EC were unavailable during this period.

The EC sonic anemometer cannot operate properly when wet, so H and LE data collected from the EC site were excluded from this study during days with rainfall. Because EC sensors were mounted to the south of the tower, data also were excluded when winds were from the north due to flow distortion through the tower (Dyer 1981). Dyer et al. (1982) suggest that flow distortion error may be as high as 20%, but the exact error remains

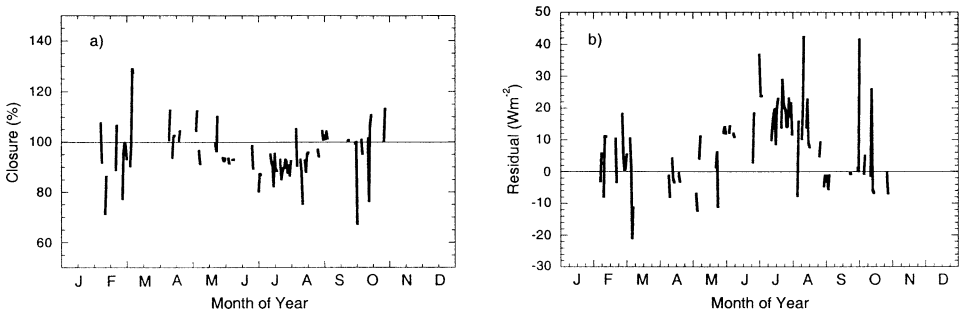

FIG. 2. At the EC site, (a) closure (%) and (b) residual (W m^{-2}) of the energy balance plotted as a function of the day of the year.

highly variable. Bowen ratio data were not used when $-2.0 < \beta < -0.5$ because small vertical gradients in temperature and moisture occasionally create spuriously large flux estimates (Ohmura 1982).

Data were collected during a 1-yr period between 1 June 1999 and 31 May 2000 from the EBBR and EC sites at Foraker. After data quality control (QC) was applied as described above, a total of 108 days were available for which all data (R_n, H, LE, and G) were complete from both EC and EBBR sites. However, much longer datasets were available for individual components of the energy budget.

3. Annual trends in closure and system differences

Data were collected from a 1-yr period characterized by a series of wet and dry spells. The months during 1999 were characterized by a wet June followed by a very dry July, August, October, and November. Temperatures remained near normal to above normal during the period. Dry weather continued through January and February of 2000, followed by much-above normal rainfall during March through May. Seasonal trends in climate and vegetation led to large but decreasing latent heat fluxes during June–August, relatively high sensible heat fluxes during the winter months, followed by increasing latent heat fluxes during the spring.

We first consider the EC site. Measurements of net radiation, ground, sensible, and latent heat fluxes were summed to produce daily totals. Closure (C) was computed as a percentage as

$$C\ (\%) = \frac{H + \mathrm{LE}}{R_n - G} \times 100, \tag{5a}$$

with 100% meaning complete closure. Closure also was computed as a residual as

$$C\ (\mathrm{W\ m^{-2}}) = R_n - G - H - \mathrm{LE}, \tag{5b}$$

with 0 W m^{-2} meaning complete closure.

The mean annual closure at the EC site at Foraker was estimated at 95.9% with a standard deviation of 10.1% and a range between 67% and 129%. The sample size included 108 days. An examination of the daily estimates of closure reflects seasonal variations (Fig. 2a). The percentage of closure decreased to minimum values during June, July, and August and which coincided with the days of greatest latent heat flux. Closure estimated as a residual (Fig. 2b) also showed a similar annual cycle with an annual mean of +7.2 W m^{-2} and a standard deviation of 11.8 W m^{-2}. The daily residual estimates ranged between −20.9 to 42.2 W m^{-2}.

The residual appears to be inversely proportional to the daily Bowen ratio ($\beta = H$/LE); that is, large, positive residuals occur when LE is large. To better determine the relationship between closure residual and the Bowen ratio, daily values of BR were estimated for the EC site from daily values of H and LE. Daily closure rates and residuals are plotted as a function of Bowen ratio in Fig. 3. A systematic decrease in closure was noted when the BR < 1.0. However, when the BR > 1.0, a rather large variance in closure of about 100% was observed. These results are consistent with those found by Barr et al. (1994) who found decreasing closure with decreasing Bowen ratio.

We now also consider the EBBR site, to help isolate reasons for nonclosure at the EC site. In Fig. 4, daily closure residuals at the EC site are plotted as a function of EC versus BR measurement system differences in observed ($R_n - G$) in Fig. 4a and observed (LE + H) in Fig. 4b. (As an aside: data from the ARM/BR SIRS were not available during much of the summer period when the residual of closure at the EC site was at its largest value. For this reason, the ARM values of R_n, and in turn the EBBR estimates of LE and H, were recomputed using EC radiation data from the CNR1. Data points in Fig. 4 from such instances are plotted as filled circles.)

As differences between the EBBR and EC observations decreased, closure rates improved. System differences in the measured available energies ($R_n - G$) were generally limited to ±10 W m^{-2} (Fig. 4a). For those days when the residual of closure was greater than 10 W m^{-2}, we may assume either an underestimate by EC in H or LE, or a combination of both. Results from McNeil and Shuttleworth (1975), Dugas et al. (1991), and Sellers and Hall (1992) also concluded that either the H and/or LE were underestimated by the eddy correlation system.

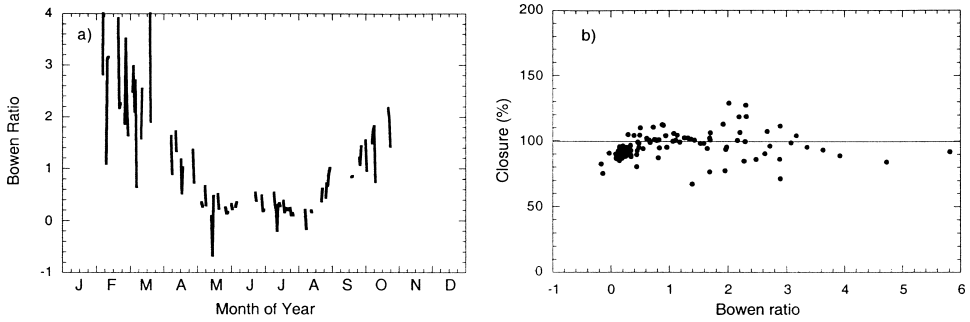

FIG. 3. At the EC site, (a) daily estimates of Bowen ratio plotted as a function of time of year, and (b) daily estimates of closure plotted as a function of daily estimates of Bowen ratio.

A similar examination of the aerodynamic fluxes (H + LE) plotted as a function of the closure residual showed EBBR − EC differences as large as 40 W m^{-2} (Fig. 4b). Linear regression of the data revealed a minimal relationship between differences in available energy versus closure ($R^2 = 0.292$). However, linear regression of the EBBR − EC difference between the total aerodynamic fluxes (LE + H) versus the EC energy residual supported a much stronger, positive correlation of 0.710 (0.451) when the CNR1 (SIRS) was used. Therefore, large positive residuals from the EC occur when (H + LE) is underestimated relative to the BR system.

a. Seasonal trends

Differences between the EC and EBBR systems were quantified for each component of the surface energy budget. Assuming the difference between the EC and EBBR methods can be linked with failure to close the energy budget, examining differences between individual components of the energy budget produced by the observing systems may conclusively identify which components are in error.

1) NET RADIATION

Four-component net radiation is measured using the CNR1 at the EC site and the SIRS at the EBBR site. The differences between the SIRS and CNR1 remained nearly steady at −5 to −10 W m^{-2} throughout the year (as shown in Fig. 5a). The remarkable stability of these two observing systems increased our confidence in the four-component measurements of R_n. This justifies the summer substitution of the CNR1 for SIRS cited earlier in section 3.

Mean differences of the EBBR Q*6.1 and EC NR-Lite ''bulk'' radiometers for R_n compared to the four-component SIRS R_n also averaged less than 10 W m^{-2}. However, long-term variations were noted. Annual trends from each system revealed significant errors (Figs. 5b,c). Instrument drift by the EBBR Q*6.1 was significant, decreasing from a difference of approximately −10 W m^{-2} in September to nearly −30 W m^{-2} by November. A dome replacement during December and a calibration correction appears to have corrected the difference based upon the Q*6.1 and SIRS data. However, data from the Q*6.1 and SIRS diverged again from near 0 W m^{-2} during January to +10 W m^{-2} by May. Differences in data from the NR-Lite and SIRS

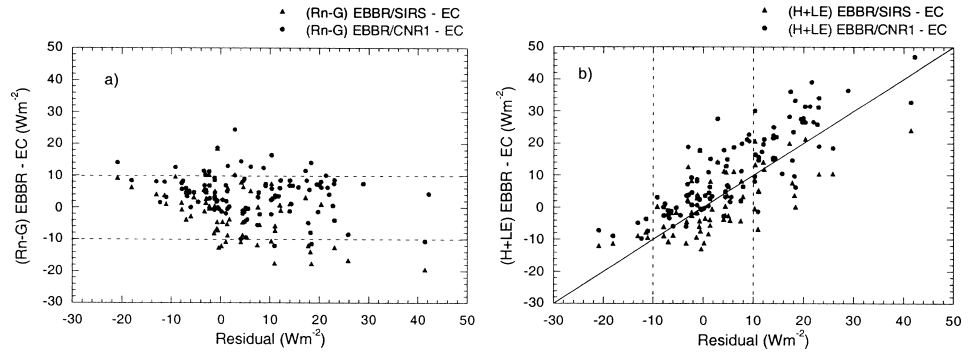

FIG. 4. Daily closure residuals at the EC site as a function of EBBR minus EC measurement differences of (a) $R_n - G$ and (b) H + LE. Filled circle data points denote when the BR calculations of R_n used EC CNR1 measurements (see text).

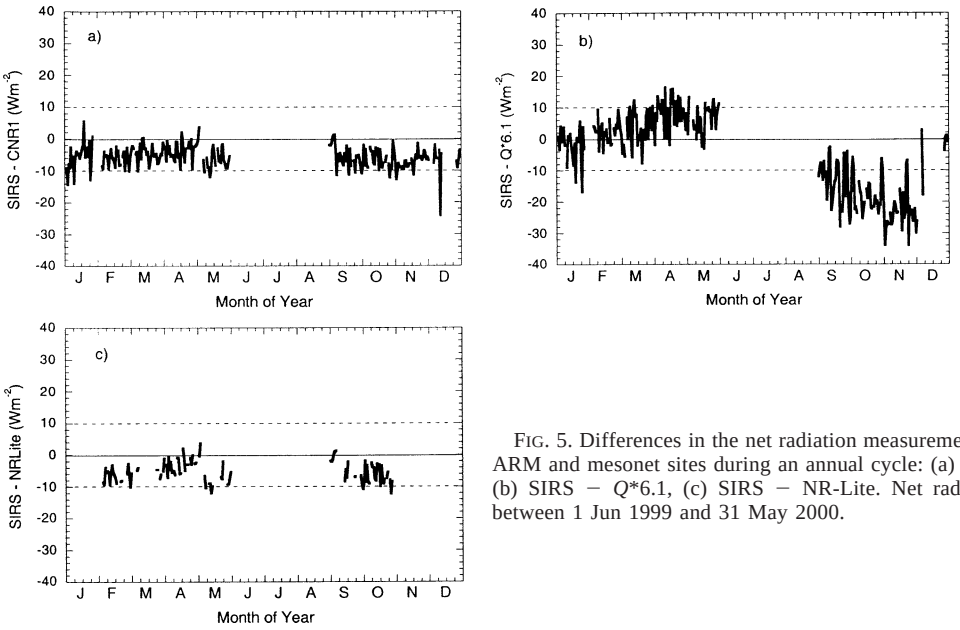

FIG. 5. Differences in the net radiation measurements between the ARM and mesonet sites during an annual cycle: (a) SIRS − CNR1, (b) SIRS − Q*6.1, (c) SIRS − NR-Lite. Net radiation collected between 1 Jun 1999 and 31 May 2000.

remained constant throughout the year. Note, however, that data from the NR-Lite were not used from days with rainfall.

2) GROUND HEAT FLUX

Daily values of the difference in ground heat flux between the EBBR and EC sites varied between ±15 W m^{-2} (Fig. 6a). The scatterplot of daily estimates of BR versus EC ground heat flux (Fig. 6b) show the EC values are greater than those from EBBR during warm days (positive daily flux) and less than EBBR estimates during the cool days (negative daily flux). The annual cycle revealed a similar trend (Fig. 6a). Differences were at a maximum during the summer months and appear related to changes in radiative forcing. These differences seem to represent real heterogeneity at the site which could limit the accuracy of closure. Section 4 further examines the sources of differences in measured ground heat flux and net radiation.

3) SENSIBLE AND LATENT HEAT FLUXES

As shown in Fig. 7a, sensible heat flux differed most between systems during the spring months, during which the EC underestimated H relative to values obtained at the EBBR site. However, during the same period, EC overestimated LE relative to EBBR (Fig. 7b). Thus, while the sum of (H + LE) was similar at both sites during this time (Fig. 8), the estimated Bowen ratios were different (see section 3b). Closure estimates from the EC method varied close to 100% (±10%) during the spring, which increased our confidence in measurements from the EC. During the spring period, the ARM EBBR system favored H flux, while the mesonet EC system favored LE flux. There is no clear physical explanation for this.

Large differences in EBBR versus EC LE flux were observed during the summer period (Fig. 7b). The EC in summer underestimated LE by as much as 40 W m^{-2} relative to values produced by the EBBR system, and

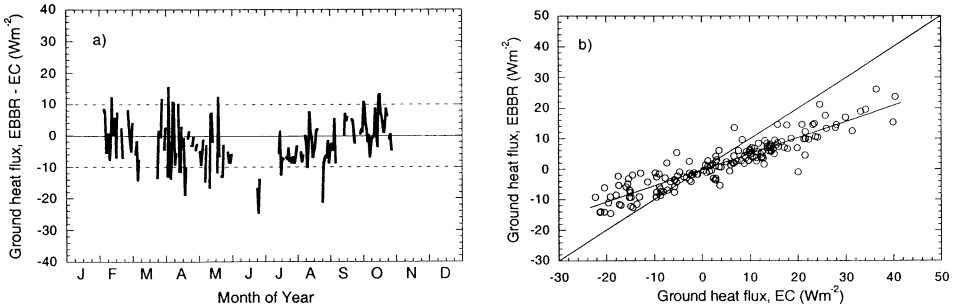

FIG. 6. (a) Differences in daily ground heat flux between the EBBR and EC sites during an annual cycle. (b) Scatterplot of BR vs EC daily totals of ground heat flux collected between 1 Jun 1999 and 31 May 2000.

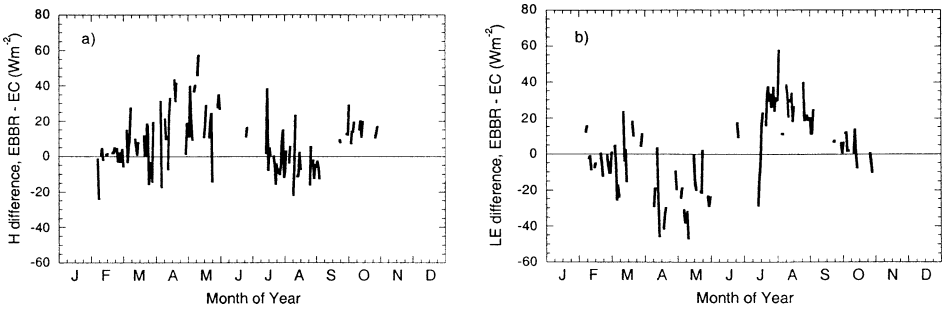

FIG. 7. Differences in daily total (a) sensible heat flux and (b) latent heat flux between the EBBR and EC sites during an annual cycle. Data were collected between 1 Jun 1999 and 31 May 2000.

unlike the spring period, EC closure estimates (Fig. 2) were consistently negative during summer. Differences in H measured by both systems remained generally less than ± 10 W m^{-2}. Despite very dry conditions during July and August, high vegetation greenness as represented by a normalized difference vegetation index (NDVI) > 0.50 resulted in large values (>150 W m^{-2}) of LE. As the soil dried during the period, LE fluxes declined, and closure improved. By September closure estimates were $\sim$100%, but by October, the closure values are big again.

Differences between the net available energy and aerodynamic fluxes using data from both sites are shown in Figs. 8a,b. Note that the difference in values of the available energy between the two sites was $\sim \pm 15$ W m^{-2} throughout the year. On the other hand, the difference in aerodynamic fluxes obtained by both systems varied between -10 and over 30 W m^{-2}. Section 5 further examines the causes of the differences between BR and EC aerodynamic fluxes.

b. Diurnal trends

Diurnal averaging of the surface fluxes from the BR and EC stations yields new insight into which component of the EC energy budget remains in error when EC closure fails. The R_n, G, H, and LE were averaged on a diurnal basis for each month during the period from 1 September 1999 through 31 May 2000.

First, R_n from the four-component radiometers and G from both the EBBR and EC sites were averaged on a monthly basis (Fig. 9). Little annual variation in the EC versus EBBR differences is noted during the 9-month period. Daily difference in net radiation between the CNR1 and SIRS changed little during the year.

Greater daytime differences between observing systems were observed in G. In fact, little correlation existed between ground flux estimates produced by the two observing systems (EBBR and EC). The EC estimates of G reach a maximum value near midday while EBBR estimates of G achieve a broad peak near dusk. Greater (more positive) values of G at the EBBR site during the night create daily differences of less than ± 10 W m^{-2} between the EBBR and EC systems (Fig. 6). The greater midday estimates of R_n at the EC site are dominated by the much larger estimates of G, resulting in lower daily averaged values of available energy when compared to similar estimates from EBBR. These significant differences in EC and EBBR G measurements are examined in more detail in section 4c.

Significant differences in the mean, monthly diurnal cycles were observed between the EBBR and EC systems in both H and LE (Fig. 10). EBBR estimates of H were much larger than EC estimates during all months, although diurnal trends were similar. Diurnal trends in the LE differed significantly, with EBBR estimates greater during the morning hours, and EC estimates greater during the afternoon period. Furthermore, a rapid increase in LE is observed at sunrise by

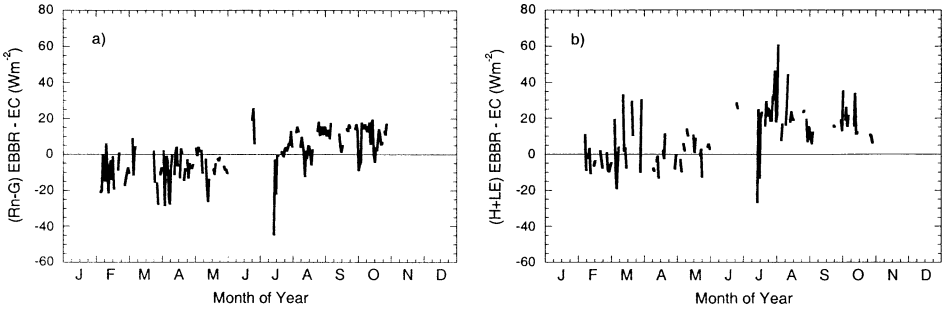

FIG. 8. Differences in (a) daily available energy ($R_n - G$) and (b) daily total aerodynamic flux (LE + H) during an annual cycle at the EBBR and EC sites.

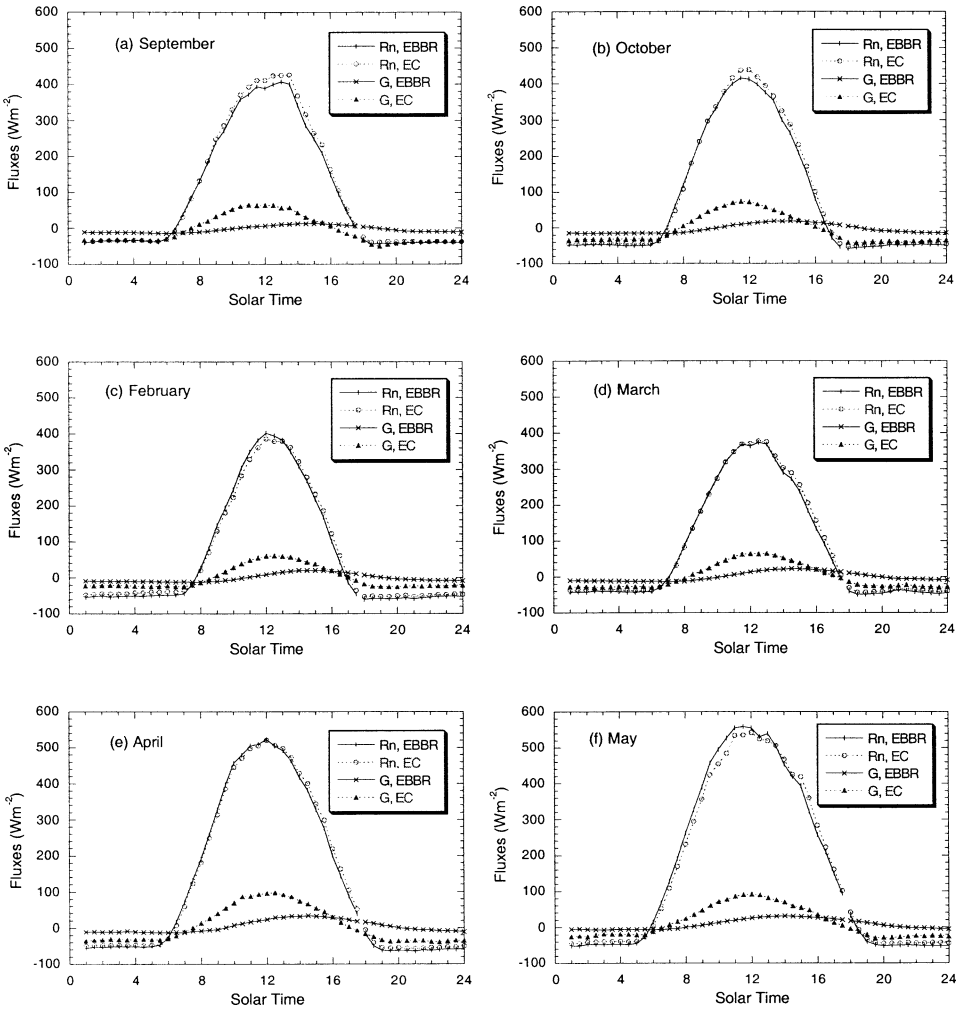

FIG. 9. Monthly mean diurnal cycle of net radiation (R_n) and ground heat flux (G) as measured at the EBBR and EC sites at Foraker for six different months during 1 Sep 1999–31 May 2000.

the EBBR system of ARM that is not captured by the EC system of the mesonet.

To minimize errors created by differences in the measurement of available energy, using Eqs. (1)–(2) the EBBR fluxes measured by ARM were rescaled (lowered) according to the lower available energy from the EC system (not shown). In this manner, all relative differences between observing systems could be attributed to the measurement of H and LE. EBBR-estimated fluxes compared significantly closer to the EC fluxes after adjustments were made to the EBBR available energy. The root mean square (rms) difference between H estimates improved from 31.9 to 11.0 W m^{-2}. Rms differences between LE estimates improved from 18.7 to 8.6 W m^{-2}.

Figure 11 gives the monthly mean diurnal cycle of EC closure in percent and EBBR minus EC difference in H and LE for six different months during the period September 1999–May 2000. A strong diurnal dependence is evident. Minimal closure is observed during the early morning periods. However, closure reaches its maximum at midday before decreasing during the late afternoon. Barr et al. (1994) detected a similar diurnal pattern in EC closure. The diurnal dependence of closure errors could be caused by dependence upon stability and fetch. Here, we define fetch as the area upwind of a site that most influences the measurement (Glickman 2000). The atmosphere is more stably stratified during the early morning and early evening periods. The size of the fetch area—as a function of wind speed, stability, and measurement height—increases by an order of magnitude during stable conditions and includes a much greater area of heterogeneity.

Minimal closure rates recorded near sunrise appear caused by an underestimate in LE as measured by the EC. Closure rates are ~100% during the mid- to late afternoon when Bowen ratios are the largest (see Fig. 12); closure rates are worst near sunrise and sunset when

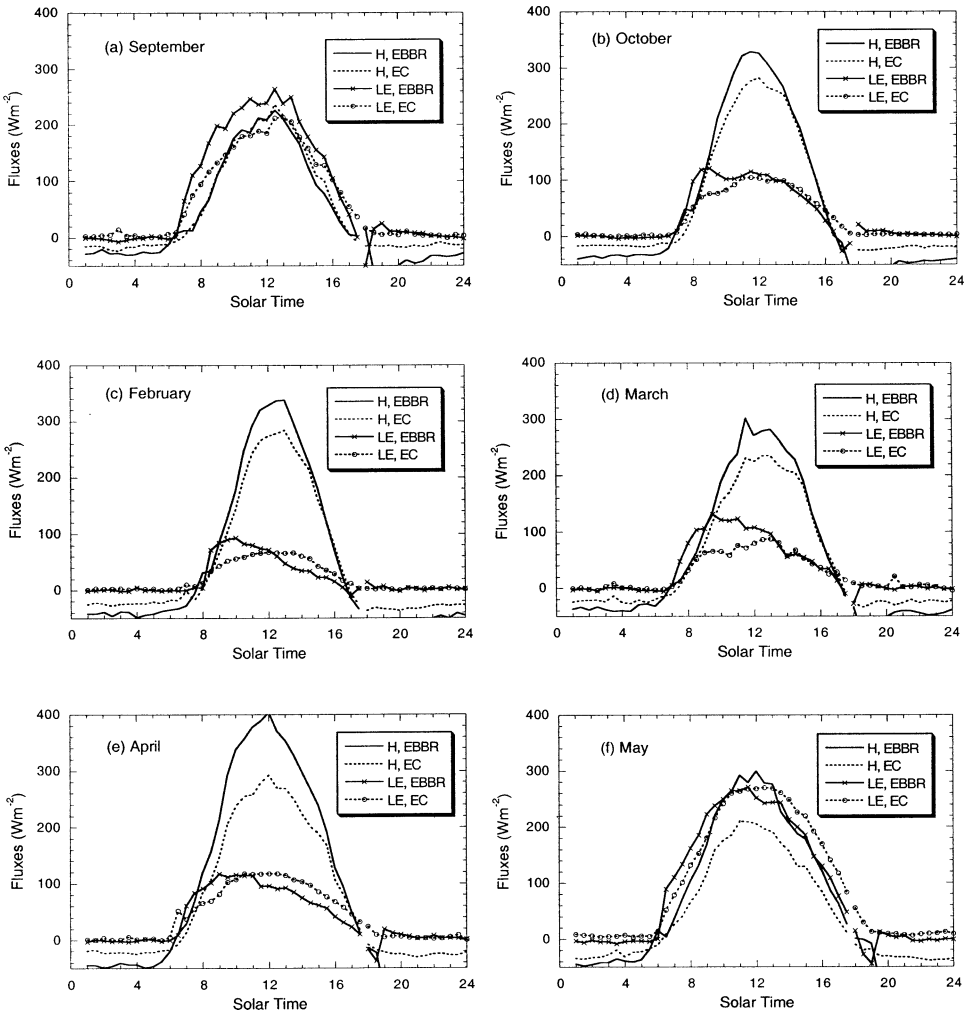

FIG. 10. Monthly mean diurnal cycle of sensible (H) and latent heat flux (LE) as estimated at the EBBR and EC sites at Foraker. The EBBR estimates of flux used the net radiation measured by the EC four-component SIRS for six different months during 1 Sep 1999–31 May 2000.

the ratio of H to LE diminishes. The errors in both diurnal and seasonal closure rates appear to result from an underestimate of the latent heat flux.

4. Causes of mesonet (EC) versus ARM (EBBR) differences in available energy ($R_n - G$)

A combination of sensor error and/or surface heterogeneity appear responsible for observed differences in available energy between the EC and EBBR systems. Two 10-day periods of data were chosen from the year-long dataset for a more detailed examination of the problem. Quiescent conditions prevailed during most of the two periods; partly to mostly clear skies dominated. Each period represented different synoptic conditions, however. The first period of data collected during 11–20 August 1999 represented an excellent ''dry-down'' period. Mostly clear and hot conditions prevailed. The second period of data, collected between 24 February and 4 March 2000, represented much wetter soil conditions. Partly to mostly sunny skies and cool temperatures prevailed along with several days of rainfall. No precipitation was recorded during the August period; data were not used when rain occurred during the February–March period. Shortwave data were not included if values were less than 10 W m^{-2}.

a. Net radiation

The four components of the radiation budget were examined during each collection period. Differences in reflected shortwave and incoming and outgoing longwave radiation between systems were relatively insignificant and well within instrument error. Only the results of observed incoming shortwave radiation are presented (Figs. 13a,b). Note that the CNR1 was replaced between test periods so that similar results may not be expected between the August and February periods.

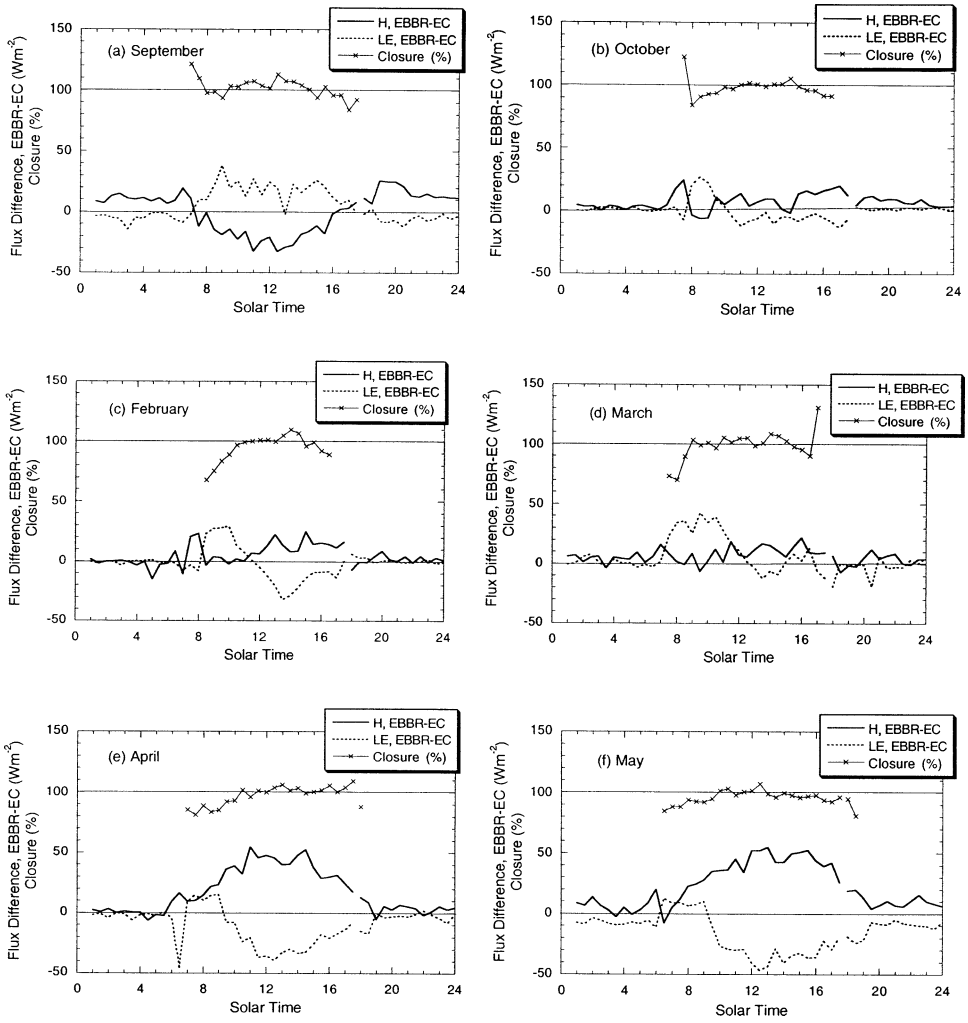

FIG. 11. The monthly mean diurnal cycle of EC closure in percent and EBBR minus EC differences in *H* and LE for six different months during 1 Sep 1999–31 May 2000. The EBBR estimates of flux used the available energy from the EC.

Differences in incoming solar radiation between the CNR1 and SIRS are plotted as a function of solar time (Figs. 13a,b). During August (Fig. 13a) some diurnal dependence was observed. The difference in shortwave radiation may be indicative of some slight calibration error by one or both sensors. The presence of this calibration error is consistent with radiation differences being symmetric about solar noon. During the February–March period (Fig. 13b), like August, differences between systems were not significant as a fraction of the incoming net radiation. However, differences in measurements of the incoming shortwave radiation were asymmetric about solar noon. Such differences could be attributed to either tilt off vertical by one of the sensors or by pyranometer heating due to radiation or both. Prior to solar noon, the CNR1 underestimated shortwave radiation relative to the SIRS system; during the afternoon, the CNR1 overestimated the radiation relative to SIRS. Thus, either the CNR1 was tilted toward the west or one component of the SIRS system was tilted to the east or both. All four components of the CNR1 are combined into a single unit; thus, no tilt error is suggested by the reflected shortwave data. Accordingly, an eastward tilt of only a few degrees by the SIRS unit could account for the incoming shortwave being underestimated.

b. Soil moisture

Next, measurements of soil moisture from the sites were compared. Soil moisture measurements are critical to understand differences in ground heat flux measurements to follow in section 4c. The August data captured a dry-down period when precipitation did not occur and a high evaporation rate was evident. On the other hand, soils during the February–March period remained nearly saturated as a result of several rain events. Direct com-

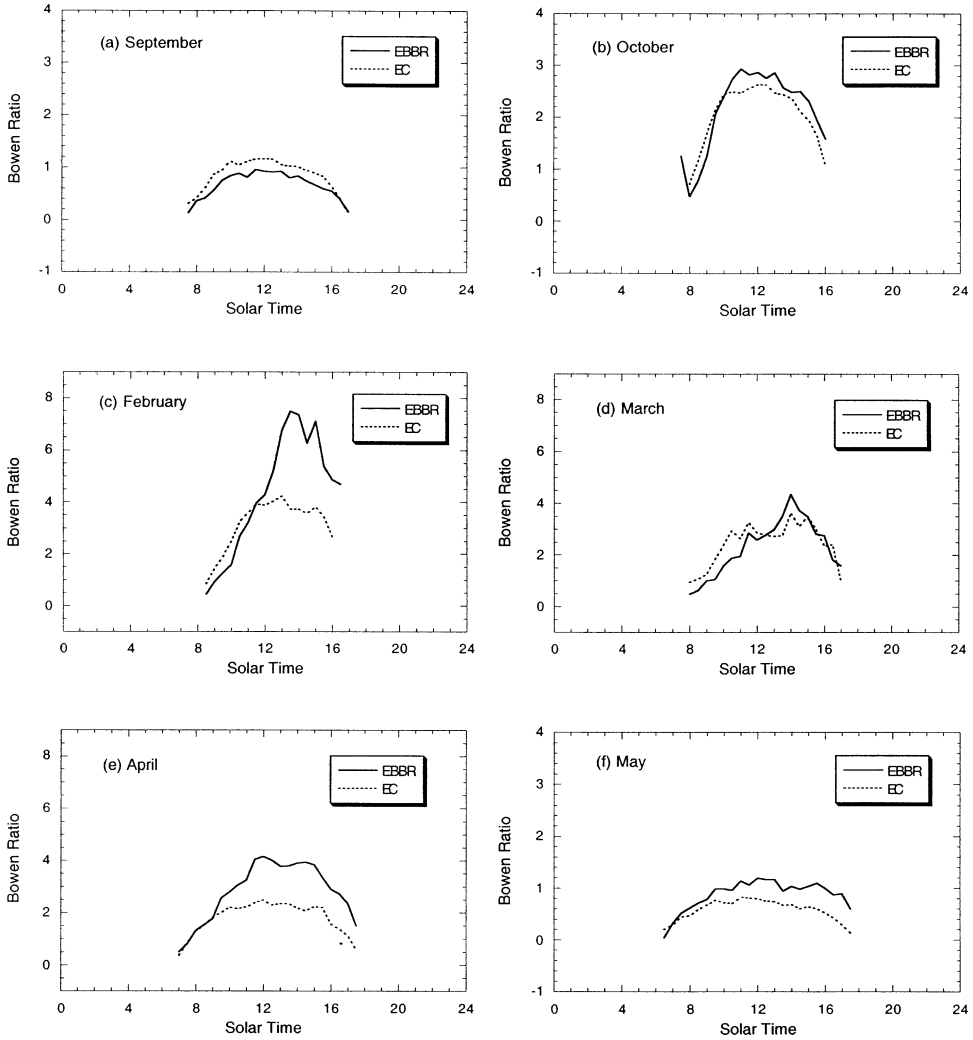

FIG. 12. The mean monthly diurnal cycles of Bowen ratio as estimated at the EBBR and EC sites at Foraker. The EBBR estimates of flux used the available energy from the EC for six different months during 1 Sep 1999–31 May 2000.

parisons of data from the EBBR and EC sites are shown for both periods in Figs. 14a–d.

Beginning with 11 August in 1999, the volumetric water content ranged between 28% and 30% as measured by the SWATS sensors; the EC sensor estimated a soil water content of 28%. By the end of the 10-day period, volumetric water content ranged between 23% and 24% between the two sites. An examination of the

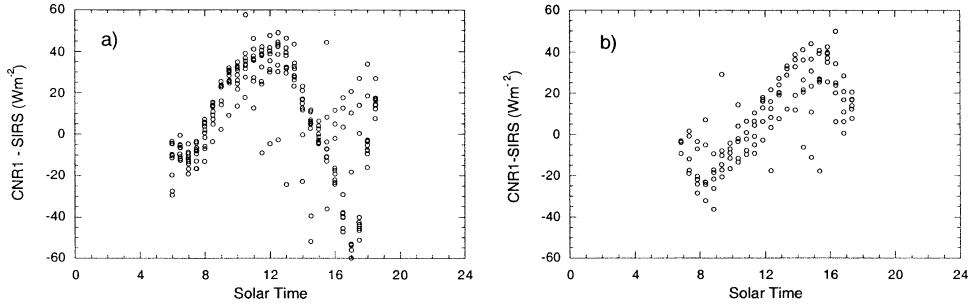

FIG. 13. The diurnal cycle of differences between the K&Z CNR1 and ARM SIRS for incoming shortwave during (a) 11–20 Aug 1999 and (b) 24 Feb–4 Mar 2000.

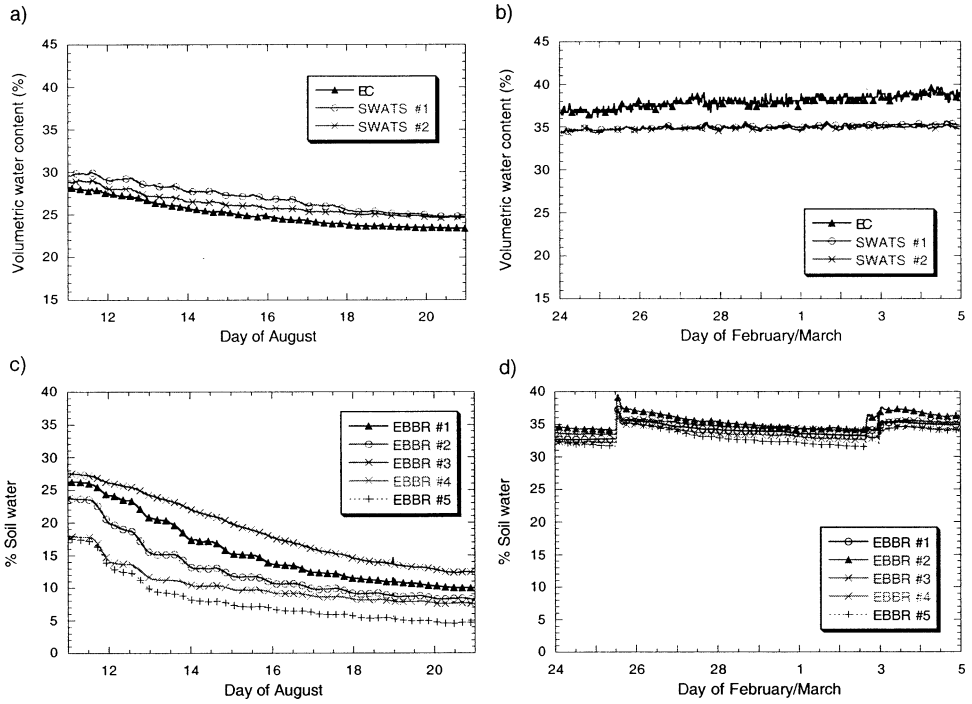

FIG. 14. Volumetric water content (%) as measured during (a) 11–20 Aug 1999 and (b) 24 Feb–4 Mar 2000. Percent soil water as measured during (c) 11–20 Aug 1999 and (d) 24 Feb–4 Mar 2000.

percent soil water as estimated by the ARM/EBBR sensors showed a range of 18%–27% on 11 August, and by 20 August, had decreased to a range between 5% and 12%. Note that the volumetric water content does not vary significantly (<3%) between the EC and SWATS sensors, spaced approximately 100 m apart. However, significant differences exist among the five EBBR sensors, spaced only 1 m apart. Furthermore, clear differences exist in the magnitude of the temporal trends between the EBBR and SWATS albeit in different units. Such differences are likely caused by differences in sensor calibration and conversion methods used (Dingman 1994; Hillel 1998). Much uncertainty remains in the accuracy of the conversion method from soil water potential to volumetric water content and percent soil water (J. Basara and K. Humes 2000, personal communication). Though it is possible that the soil moisture from EBBR is more representative of the soil moisture at the ARM site, such differences between the EC/SWATS and EBBR sensors are most likely not due to soil heterogeneity because of the very similar results from the EC and SWATS measurements, which use the same type sensor and calibration and conversion methods.

The spring period remained saturated with soil water content ranging between 30% and 40% (Figs. 14b,d). The EC and SWATS observations did not respond as quickly to rain events as did the sensors from EBBR. This difference most likely results from the fact that the EBBR sensors were buried at 2.5 cm while the EC and SWATS sensors were installed at a 5-cm depth. Variations in ground cover also could have had some impact.

The soil heat capacity is computed as a direct function of the heat capacity (C) and volume fraction (X) of minerals (m), organic matter (o), water (w), and air (a) of the soil, as defined by Fritschen and Gay (1979):

$$C = X_m C_m + X_o C_o + X_w C_w + X_a C_a. \quad (6)$$

Of the variables in Eq. (6), only the volume fraction of water varies significantly as a function of time. The soil heat capacities have been computed for the soil moisture estimates from the EC and SWATS data; soil heat capacities were provided by ARM for the EBBR data. Soil heat capacities from EBBR, SWATS, and EC all are computed as a function of the soil moisture (Fig. 15). Such low estimates of soil moisture from the EBBR site ''create'' much lower estimates of soil heat capacity when compared to similar data from SWATS and EC.

c. Ground heat flux

The soil heat flux at the bottom of the 5-cm soil layer, the integrated 0–5-cm soil temperature, and the ground heat flux were compared using data from the EBBR and EC systems. The soil moisture measured at both sites was compared in section 4b because the soil moisture strongly modulates the heat capacity C in Eq. (1) and hence the heat storage term.

Layer-bottom soil heat flux is measured at the EC and EBBR sites using the same model of heat flux plate, the

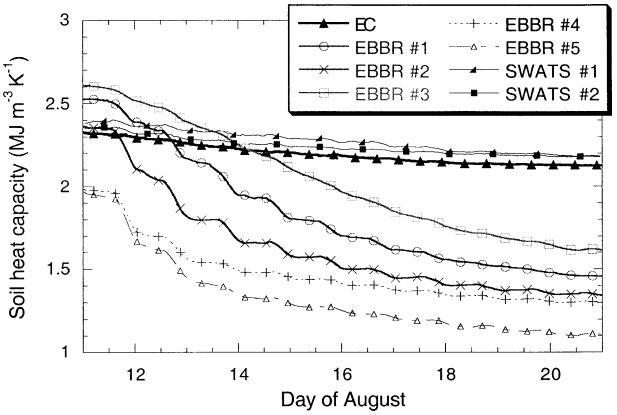

FIG. 15. Daily average values of soil heat capacity estimated as a function of soil moisture data collected from EC, EBBR, and SWATS. Data were collected from 11–20 Aug 1999.

HFT3.1 manufactured by REBS. Two sensors were installed 1 m apart at the EC site, while five sensors were installed 1 m apart at the EBBR site. All sensors were installed at a depth of 5 cm. Data from all seven plates obtained during August 1999 are plotted in Fig. 16.

Despite using the same instruments, large differences in measurements are noted between sites (Fig. 16a). The August data revealed that the five sensors installed at the EBBR facility provided data with a damped diurnal cycle and a daily maximum layer-bottom soil heat flux of ~20 W m^{-2}. The EC sensors produced data containing daily peak values of 60–80 W m^{-2}. Nighttime values from the two EC sensors reached a minimum of −20 to −40 W m^{-2} while EBBR sensors reached nighttime minimums of 0 to −10 W m^{-2} (Fig. 16b). The February–March data were strikingly similar (not shown).

Significantly large differences (>5°C) were also noted between sites in measurements of the integrated 0–5-cm soil temperature (Fig. 17a). The daily amplitude of soil temperature at the EBBR site varied between 2° and 3°C; the daily amplitude of the soil temperature at the EC site varied by as much as 7°–10°C (Fig. 17b). Results were similar for the February–March data.

The much larger amplitude of layer-bottom soil heat flux and layer-integrated soil temperature at the EC site likely results from a distinct difference in soil and/or vegetation characteristics. A thicker and denser vegetation cover at the EBBR site would produce a damped diurnal cycle while less vegetation and more bare soil at the EC site would yield a diurnal cycle with a larger amplitude. However, a visual inspection did not indicate noteworthy differences in vegetation between the sites. Dense vegetation covered sensors at both sites. In addition, differences between systems did not vary with seasonal changes in vegetation. Variations in the layer-bottom soil heat flux and the layer-integrated temperature also could be caused by differences in soil type. The soil type at the EBBR site is classified as silt loam; the EC site has been classified as sandy loam. The large diurnal cycle of layer-bottom soil heat flux and layer-integrated soil temperature at the EC site is consistent with that expected from a sandy soil. Nevertheless, the large differences in soil heat flux and temperature indicate the difficulty and uncertainty in soil measurements, even when the same type of instrument is used.

The change in the energy storage in the soil between 0 and 5 cm [second term of rhs of Eq. (4)] was calculated for the EC and EBBR sites (Fig. 18). The storage term is simply a function of the soil heat capacity and time change in soil temperature. The daily amplitude of soil heat storage at the EC site is over 100 W m^{-2} while the EBBR site daily amplitude remains less than 10 W m^{-2}. The two 10-day time series and mean daily amplitudes of the total ground heat flux estimates are shown in Fig. 19 from both EC and EBBR. Again, the large daily amplitude observed at the EC site is much reduced at the EBBR location.

A review of Figs. 16 and 18 finds that differences between the EC and EBBR estimates of the layer bottom soil heat flux and the change in energy storage are both significant and comparable in magnitude. Whereas both the soil heat capacity (Fig. 15) and the layer-integrated soil temperature (Fig. 17) contribute to the change in energy storage, the layer-integrated soil temperature dominates the term as evidenced by system differences.

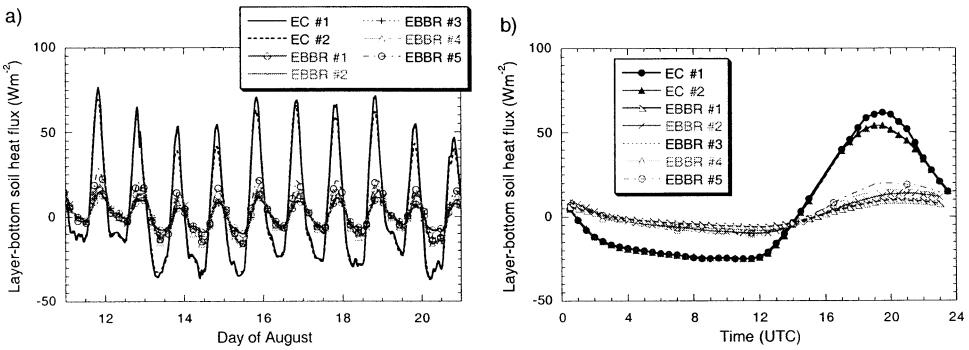

FIG. 16. (a) Time series and (b) 10-day diurnal average of the layer-bottom soil heat flux (W m^{-2}) at 5-cm depth as measured by seven heat flux plates (two at EC site, five at BR site) during 11–20 Aug 1999.

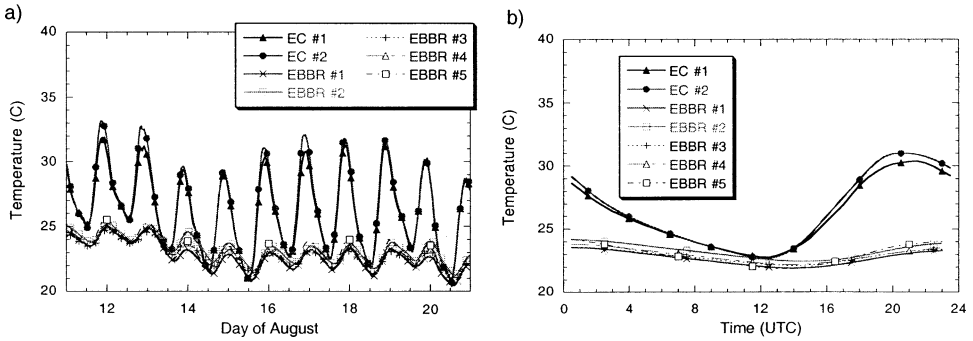

FIG. 17. (a) Time series and (b) 10-day diurnal average of the integrated soil temperature (°C) between 0 and 5 cm as measured by the seven heat flux plates 11–20 Aug 1999.

The soil heat capacities at each site are within 33% of one another, but the change in the layer-integrated soil temperature with time, dT/dt, is four times greater at the EC site than measured at the EBBR site. While sensor error is one explanation, the observed differences in the layer-integrated soil temperature between the EC and EBBR systems are most likely real.

5. Causes of mesonet versus ARM differences in latent and sensible heat fluxes

If surface heterogeneity exists across an area of less than 100 m in width, the accurate measurement and modeling of the surface budget across a heterogeneous landscape could be difficult to achieve. In fact, when such heterogeneity exists, then measurement of the available energy at a single tower cannot represent the larger scale region.

One possible cause for observed differences in the aerodynamic fluxes between systems may be due to the theoretical assumptions imposed by the BR system. The BR technique assumes the eddy diffusivities of heat and water vapor are equal ($K_h = K_w$). Several studies determined that $K_h \neq K_w$ during stable and neutral conditions (Motha et al. 1979; Lang et al. 1983; Dugas et al. 1991).

Lang et al. (1983) determined a method to study eddy diffusivities when both BR and EC methods were available. The definitions used by Lang et al. are

$$K_H = \frac{-H}{\left(\rho C_p \dfrac{\partial \theta}{\partial z}\right)} \tag{7a}$$

$$K_w = \frac{\lambda E}{\left(\rho \lambda \dfrac{\partial Q}{\partial z}\right)} \tag{7b}$$

$$H = \rho C_p \overline{w\theta} \tag{8a}$$

$$\lambda E = \rho \lambda \overline{wq}. \tag{8b}$$

Bowen ratios of gradient (β_g) and flux (β_f) are formed from Eqs. (7) and (8), as

$$\beta_g = \frac{C_p \Delta \theta}{\lambda \Delta Q} \quad \text{and} \tag{9a}$$

$$\beta_f = \frac{C_p \overline{w\theta}}{\lambda \overline{wq}}. \tag{9b}$$

Lang et al. demonstrated how the ratio of eddy diffusivities of heat to vapor equals the Bowen ratio of flux to gradient as defined by Eqs. (8):

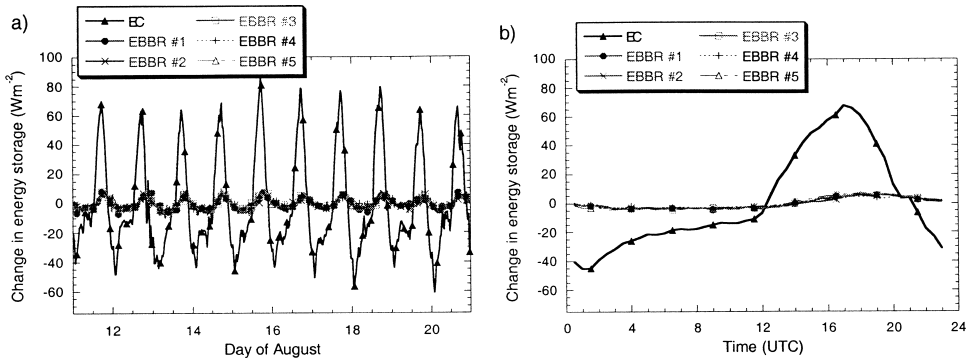

FIG. 18. (a) Time series and (b) 10-day diurnal average of the change in energy storage (W m^{-2}) as measured during 11–20 Aug 1999.

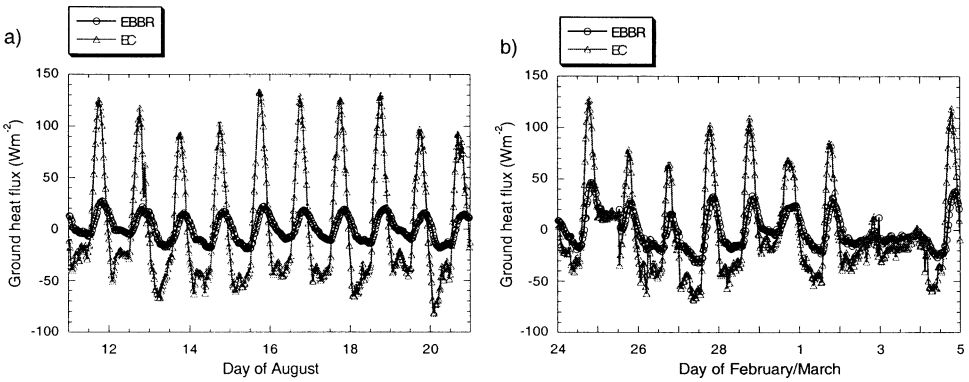

FIG. 19. The time series of the total ground heat flux (W m^{-2}) as measured during (a) 11–20 Aug 1999 and (b) 24 Feb–4 Mar 2000.

$$\frac{K_H}{K_W} = \frac{\beta_f}{\beta_g}. \tag{10}$$

Because closure is near 100% during midday, the EBBR and EC methods can be used to determine the behavior of the eddy diffusivities. For five of the six months shown in Fig. 12, the midday observations show that the Bowen ratio measured by the gradient BR method (in this case, β_g) is greater than the Bowen ratio measured from the EC method (β_f), or $\beta_g > \beta_f$. Thus, from Eq. (10), $K_W > K_H$. Lang et al. demonstrated that $K_W > K_H$ during stable conditions due to either decoupling of temperature and humidity within the vertical profile or due to the relatively small depth of the developing layer. However, the observed conditions at midday are unstable, and thus reasons for $K_W > K_H$ cannot be readily explained.

A second feature observed in the diurnal cycles of flux (Figs. 10 and 11) is the rapid increase in latent heat flux at sunrise. This sudden jump in flux is particularly noteworthy during October, February, and March. The EC method often fails to measure this rapid increase, and failure to capture this feature results in a repeated underestimate of closure at sunrise. As shown in Fig. 11, closure is often at its worst near sunrise and near sunset. This problem appears to be common to all ten OASIS super sites (Brotzge 2000). This problem begets two questions: 1) Why does the EC method fail to measure a sudden increase in latent heat? 2) Is this rapid increase in LE flux real? If not, then is the BR method simply appropriating the available energy into its subsequent aerodynamic fluxes?

One possible cause of divergent behavior between observing systems arises from the height at which the sensors are located. The BR system is closer to the ground and any vertical moisture gradient is sampled between 2 and 3 m. The sonic anemometer and krypton hygrometer of the EC system are mounted at a height of 4.5 m AGL. During the early morning hours, a stable boundary layer is dominant and an inversion could set up between 2 m and 4.5 m. Low-level moisture gradients very near the surface could be detected by the Bowen ratio system but missed by the EC technique due to fetch differences.

Tanner (1988) demonstrated how changes in surface properties upwind of an observing site create significant differences in Bowen ratio with height. Tanner mounted two sonic systems 4 m apart at a height of 1.35 m AGL. The ground surface directly beneath his sensors was wheat stubble; however, a soybean field was upwind of his site. The two sonic systems measured nearly the same Bowen ratio. On the third day of data collection, the second sonic system was lowered to a height of 0.9 m. At this point, the second system measured a greater Bowen ratio because the system at 1.35 m was affected by the LE flux advected from the soybean field. On the other hand, the system at 0.9 m was dominated by sensible heat flux from the wheat stubble.

6. Conclusions

The purpose of this research was to identify problems associated with closure of the surface energy budget. Several sources were found, all of which adversely affect closure. First, instrumentation error among net radiometers and soil moisture sensors was found, which lead to greater uncertainty in R_n and G. Second, heterogeneity of soil characteristics combined with instrument uncertainty in measuring soil temperature and below-ground soil heat flux also contributed to large site differences in G. Such variability questions the spatial representativeness of point-scale measurements of G. Third, underestimates of LE by EC (when compared to BR estimates) tended to coincide with closure less than 100%. Thus, while large positive or negative variations in closure could occur as a result of sensor error and surface heterogeneity, closure was systematically lowered by an underestimate in LE.

Instrument error accounted for some variability in closure. While little annual variation was noted between the four-component radiometers, several problems with the net radiometers were detected. Significant variability (15%) in the EBBR percent soil water estimates lead to much greater uncertainty in EBBR estimates. Sensor

inaccuracy, bias, and calibration and conversion errors contribute to degrade observational performance.

Results shown in Figs. 16–17 indicate measured differences in both the layer-bottom soil flux and soil temperature between systems. While a thicker vegetation cover at the EBBR site would explain the dampened daily cycle, such site differences did not change with season. Thus, the most likely cause for differences in G is due to differences in soil type and texture. A sandier soil at the EC site is consistent with a much greater daily variability in soil heat flux.

Closure at the EC site varied seasonally, with a mean annual closure of 95.9% $\pm$ 10.1% (Fig. 2). In general, the minimum closure rates during the year occurred when latent heat flux estimates were greatest (Fig. 3). The minimum closure rates observed daily by the EC system coincided with a lower estimate of latent heat flux when compared to the ARM BR system. Daily underestimates in closure appear to result from a failure by the EC system to correctly measure early-morning and late-afternoon latent heat flux (Fig. 11). Closure approached 100% after boundary layer mixing during the late morning and afternoon. Closure was observed to be lowest during stable and transitional periods during the early morning and late afternoon.

An examination of closure from EC also may have identified a problem with the BR method. Both the annual time series (Fig. 7) and monthly diurnal cycles (Fig. 11) of H and LE showed that the EBBR method favored a partitioning into H while the EC system favored LE, when closure was near 100%. A direct comparison of the EC and EBBR Bowen ratios (Fig. 12) indicate that the EBBR Bowen ratio was often higher during mid- and late afternoon. During September, however, EC measured a slightly greater Bowen ratio. Because of the inconsistency between September and the following months, it is still unknown whether surface heterogeneity, instrument error, or erroneous theoretical assumptions behind the BR method could have created the differences in the estimates of the Bowen ratio. More work needs to be done to determine the exact causes for these differences.

Results from this study highlight the importance of instrument accuracy, site representativeness, and theoretical assumptions to measurement of surface fluxes. Using data from a single site for model and satellite validation can pose serious implications given the measurement uncertainty and surface heterogeneity found in this study. However, such problems can be minimized if care is taken to address these issues. Thus, the authors strongly recommend that redundant instrumentation be used when possible to minimize sensor errors and the effects of surface heterogeneity. For example, multiple four-component radiometers increased confidence in the net radiation measurements; likewise, data from the Q*6.1 and NR-Lite radiometers were flagged during certain periods because instrument drift was identified. Data from the ground flux sensors indicated surface heterogeneity between the two systems. Whereas the redundant ground flux sensors within a given site provided nearly identical observations, the same ground flux sensors (albeit installed at different times and with possibly different calibration) located at the two different sites yielded substantially different observations. Increasing the number of ground flux sensors within a site did not change the results from that system. These observations indicate that ground flux sensors should perhaps be spaced much further apart to better account for spatial heterogeneity. Furthermore and as demonstrated by this study, collocated EC and BR systems are suggested to aid in identifying problems when estimating H and LE.

It is also recommended that closure be included as a routine tool for quality assurance of surface data. Significant variations from 100% of closure indicate a problem with measurement of one or more components of the energy budget. For example, in this study, estimates of minimal closure by the EC method during the early morning reflected periods when the latent heat flux was underestimated.

Finally, quantifying nearby biophysical parameters is essential and should include vegetation type and height, NDVI, soil type, and land use to properly understand the context in which measurements are made. A greater understanding of site properties aids in interpreting problems with nonclosure and other data irregularities.

Acknowledgments. This research was made possible, in part, by the NSF Grant 125-5645. We would like to recognize the cooperation of the U.S. Department of Energy as part of the Atmospheric Radiation Measurement Program. The authors would like to thank Dr. Scott Richardson, Sherman Fredrickson, David Grimsley, James Kilby, and the technical support provided by the Oklahoma Climatological Survey for their professional assistance in maintenance, ingest, and quality control of the Mesonet data. Furthermore, the authors are indebted to Drs. Claude Duchon, Mike Richman, David Stensrud, May Yuan, Ken Mitchell, and two anonymous reviewers for their significant contributions and invaluable suggestions in shaping this manuscript.

APPENDIX

Derivation of the Ground Heat Flux Equation

First, we adopt the sign convention wherein soil depth, z, is positive and increases downward from the ground surface. Vertical integration of the soil column then proceeds from the top of the soil column, $z = z_1 = 0$, to the bottom of the soil column, $z = z_2 > 0$. Second, the physical parameters C and λ are as defined in section 2b(3).

The fundamental governing equation for the temporal change in soil temperature, T(K), at depth z in terms of the vertical gradient of heat flux is

$$C\frac{dT}{dt} = -\frac{dF}{dz}, \tag{A1}$$

where F (W m^{-2}) is the vertical heat flux, positive if downward. Typically during midday, the heat flux is downward (positive) and decreases with depth (increasing z), and thus the temperature rises. Integration of (A1) from $z = z_1 = 0$ to $z = z_2 > 0$ (soil layer bottom) yields

$$\int_{z=z_1=0}^{z=z_2} \left(C\frac{dT}{dt}\right) dz = -\int_{z=z_1=0}^{z=z_2} \frac{dF}{dz}\, dz. \tag{A2}$$

Next, we apply the mean value theorem of calculus to the left side of (A2) to obtain

$$\overline{\left(C\frac{dT}{dt}\right)}^{z_2} \int_{z=z_1=0}^{z=z_2} dz = -\int_{z=z_1=0}^{z=z_2} dF, \tag{A3}$$

where the overbar denotes the vertical mean over depth z_2. Further integration yields

$$\overline{\left(C\frac{dT}{dt}\right)}^{z_2} \times z_2 = -[(F)_{z_2} - (F)_{z=0}]. \tag{A4}$$

Next, we introduce "G" to denote the ground heat flux—that is, the heat flux F at the ground surface ($z = 0$)—and we substitute the following common empirical law for the heat flux F at depth $z = z_2$:

$$(F)_{z=z_2} = \left(-\lambda\frac{dT}{dz}\right)_{z=z_2}, \tag{A5}$$

which gives the heat flux at finite depth below ground as proportional to the temperature gradient at that depth, in the direction of decreasing temperature. These substitutions in (A4) yield

$$\overline{\left(C\frac{dT}{dt}\right)}^{z_2} \times z_2 = \lambda\frac{dT}{dt}\bigg|_{z_2} + G. \tag{A6}$$

Algebraically solving for G gives

$$G = -\lambda\frac{dT}{dz}\bigg|_{z_2} + z_2\overline{\left(C\frac{dT}{dt}\right)}^{z_2}. \tag{A7}$$

If we assume the heat capacity, C, is invariant across the soil layer, then we finally arrive at

$$G = -\lambda\frac{dT}{dz_1}\bigg|_{z_2} + z_2 C\left(\frac{d\overline{T}}{dt}\right). \tag{A8}$$

REFERENCES

Barr, A. G., K. M. King, T. J. Gillespie, G. Den Hartog, and H. H. Neumann, 1994: A comparison of Bowen ratio and eddy correlation sensible and latent heat flux measurements above deciduous forest. *Bound.-Layer Meteor.,* **71,** 21–41.

Brock, F. V., K. C. Crawford, R. L. Elliott, G. W. Cuperus, S. J. Stadler, H. L. Johnson, and M. D. Eilts, 1995: The Oklahoma Mesonet: A technical overview. *J. Atmos. Oceanic Technol.,* **12,** 5–19.

Brotzge, J. A., 2000: Closure of the surface energy budget. Ph.D. dissertation, University of Oklahoma, Norman, OK, 208 pp.

——, S. J. Richardson, K. C. Crawford, T. W. Horst, F. V. Brock, K. S. Humes, Z. Sorbjan, and R. L. Elliott, 1999: The Oklahoma Atmospheric Surface-Layer Instrumentation System (OASIS) Project. Preprints, *13th Conf. on Boundary Layer Turbulence,* Dallas, TX, Amer. Meteor. Soc., 612–615.

——, ——, and C. M. McAloon, 2001: The OASIS Project network for monitoring the surface energy budget. Preprints, *11th Symp. on Meteor. Observations and Instrumentation,* Albuquerque, NM, Amer. Meteor. Soc., 66–71.

Dingman, S. L., 1994: *Physical Hydrology.* Prentice Hall, 575 pp.

Dugas, W. A., L. J. Fritschen, L. W. Gay, A. A. Held, A. D. Matthias, D. C. Reicosky, P. Steduto, and J. L. Steiner, 1991: Bowen ratio, eddy correlation, and portable chamber measurements of sensible and latent heat flux over irrigated spring wheat. *Agric. For. Meteor.,* **56,** 1–20.

Dyer, A. J., 1981: Flow distortion by supporting structures. *Bound.-Layer Meteor.,* **20,** 243–251.

——, and Coauthors, 1982: An international turbulence comparison experiment (ITCE 1976). *Bound.-Layer Meteor.,* **21,** 181–209.

Field, R. T., L. J. Fritschen, E. T. Kanemasu, E. A. Smith, J. B. Stewart, S. B. Verma, and W. P. Kustas, 1992: Calibration, comparison, and correction of net radiation instruments used during FIFE. *J. Geophys. Res.,* **97,** 18 681–18 695.

Fritschen, L. J., and L. W. Gay, 1979: *Environmental Instrumentation.* Springer-Verlag, 216 pp.

——, and J. R. Simpson, 1989: Surface energy and radiation balance systems: general description and improvements. *J. Appl. Meteor.,* **28,** 680–689.

——, P. Qian, E. T. Kanemasu, D. Nie, E. A. Smith, J. B. Stewart, S. B. Verma, and M. L. Wesely, 1992: Comparisons of surface flux measurement systems used in FIFE 1989. *J. Geophy. Res.,* **97,** 18 697–18 713.

Glickman, T. S., Ed., 2000: *Glossary of Meteorology.* 2d ed. Amer. Meteor. Soc., 855 pp.

Hillel, D., 1998: *Environmental Soil Physics.* Academic Press, 771 pp.

Kaimal, J. C., and J. E. Gaynor, 1991: Another look at sonic thermometry. *Bound.-Layer Meteor.,* **56,** 401–410.

Lang, A. R. G., K. G. McNaughton, C. Fazu, E. F. Bradley, and E. Ohtaki, 1983: Inequality of eddy transfer coefficients for vertical transport of sensible and latent heats during advective inversions. *Bound.-Layer Meteor.,* **25,** 25–41.

Lloyd, C. R., P. Bessemoulin, F. D. Cropley, A. D. Culf, A. J. Dolman, J. Elbers, B. Heusinkveld, J. B. Moncrieff, B. Monteny, and A. Verhoef, 1997: A comparison of surface fluxes at the HAPEX-Sahel fallow bush sites. *J. Hydrol.,* **188–189,** 400–425.

Massman, W. J., 1993: Errors associated with the combination method for estimating soil heat flux. *Soil Sci. Soc. Amer. J.,* **57,** 1198–1202.

McNeil, D. D., and W. J. Shuttleworth, 1975: Comparative measurements of the energy fluxes over a pine forest. *Bound.-Layer Meteor.,* **9,** 297–313.

Motha, R. P., S. B. Verma, and N. J. Rosenberg, 1979: Exchange coefficients under sensible heat advection determined by eddy correlation. *Agric. Meteor.,* **20,** 273–280.

Ohmura, A., 1982: Objective criteria for rejecting data for Bowen Ratio flux calculations. *J. Appl. Meteor.,* **21,** 595–598.

——, and Coauthors, 1998: Baseline Surface Radiation Network (BSRN/WCRP): New precision radiometry for climate research. *Bull. Amer. Meteor. Soc.,* **79,** 2115–2136.

Schotanus, P., F. T. M. Nieuwstadt, and H. A. R. De Bruin, 1983: Temperature measurements with a sonic anemometer and its application to heat and moisture fluxes. *Bound.-Layer Meteor.,* **26,** 81–93.

Sellers, P. J., and F. G. Hall, 1992: FIFE in 1992: Results, scientific

gains, and future research directions. *J. Geophys. Res.*, **97,** 19 091–19 109.

Shuttleworth, W. J., and Coauthors, 1984: Eddy correlation measurements of energy partition for Amazonian forest. *Quart. J. Roy. Meteor. Soc.*, **110,** 1143–1162.

Stannard, D. I., J. H. Blanford, W. P. Kustas, W. D. Nichols, S. A. Amer, T. J. Schmugge, and M. A. Weltz, 1994: Interpretation of surface flux measurements in heterogeneous terrain during the Monsoon '90 experiment. *Water Res. Res.*, **30,** 1227–1239.

Stokes, G. M., and S. E. Schwartz, 1994: The Atmospheric Radiation Measurement (ARM) Program: Programmatic background and design of the Cloud and Radiation Test Bed. *Bull. Amer. Meteor. Soc.*, **75,** 1201–1221.

Stull, R. B., 1988: *An Introduction to Boundary Layer Meteorology*. Kluwer Academic, 666 pp.

Tanner, B. D., 1988: Use requirements for Bowen ratio and eddy correlation determination of evapotranspiration. *Planning Now for Irrigation and Drainage in the 21st Century*, R. DeLynn Hay, Ed., ASCE, 782 pp.

Tanner, C. B., 1960: Energy balance approach to evapotranspiration from crops. *Soil Sci. Soc. Amer. Proc.*, **24,** 1–9.

——, E. Swiatek, and J. P. Greene, 1993: Density fluctuations and use of the Krypton hygrometer in surface flux measurements. *Irrigation and Drainage Systems*, Park City, UT, Irrigation and Drainage Division/ASCE, 945–950.

Twine, T. E., W. P. Kustas, J. M. Norman, D. R. Cook, P. R. Houser, T. P. Meyers, J. H. Prueger, and P. J. Starks, 2000: Correcting eddy covariance flux underestimates over a grassland. *Agric. For. Meteor.*, **103,** 279–300.

Webb, E. K., G. I. Pearman, and R. Leuning, 1980: Correction of flux measurements for density effects due to heat and water vapour transfer. *Quart. J. Roy. Meteor. Soc.*, **106,** 85–100.